Contract No.:

This manuscript has been authored by Battelle Savannah River Alliance (BSRA), LLC under Contract No. 89303321CEM000080 with the U.S. Department of Energy (DOE) Office of Environmental Management (EM).

Manuscript IPVP-D-22-00394

A Parametric Finite Element Study for Determining Burst Strength of Thin and Thick-Walled Pressure Vessels

William R. Johnson[a*], Xian-Kui Zhu[a], Robert Sindelar[a], and Bruce Wiersma[a]
[a] Savannah River National Laboratory, Aiken, SC 29803

Abstract: To accurately predict the burst strength of both thin and thick-walled pressure vessels (PVs), a parametric study of PV burst strength was performed for a wide range of vessel geometries and materials using elastic-plastic finite element analysis (FEA). A valid FEA model was established through a detailed study of 2D versus 3D FEA models, the critical stress failure criterion versus the limit load criteria, and the thick-wall effect on the FEA simulations. The results show that the stresses and strains at the mean diameter, rather than outside diameter, determines a more accurate burst strength for both thin and thick-walled PVs. On this basis, a parametrized FEA script using the ABAQUS Python application programming interface (API) was used to create a large database of PV burst strengths for a variety of vessel geometries and materials, demonstrating that Python scripting is a powerful technique for performing parametric studies or generating large databases. From the FEA results, using the regression method, a new burst pressure model was developed as a function of the vessel geometry (D/t ratio) and material properties (UTS and n). As validated by a large number of full-scale burst test data, the proposed burst model can very accurately predict the burst strength for both thin and thick-walled PVs.

Keywords: pressure vessel, pipeline, burst strength, finite element analysis, strength theory, linear regression.

1. Introduction

The importance of pressure vessels (PVs) in modern technology arose as a result of the industrial revolution and the development of the steam engine. They have been extensively utilized in the energy sector. Early efforts to manufacture and use PVs (boilers) for the steam engine resulted in frequent explosions and claimed the lives of a number of people. This led to legislation and operational and design guidelines for PVs. The American Society of Mechanical Engineers (ASME) developed its Boiler and Pressure Vessel Code (BPVC) as a codified version of these early rules [1].

One of the key design factors to ensuring PV integrity is the accurate determination of ultimate pressure capability or burst strength. Over the years, a large amount of analytical, numerical, and experimental investigations have been performed for determining the burst strength of cylindrical PVs or pipes and many approximate or empirical burst pressure models were developed [2 – 4]. Law and Bowie [2] reviewed and compared 23 different models of thin-walled PV burst pressure, while Christopher et. al. [3] evaluated 12 different burst models for both thin- and thick-walled PVs.

* Corresponding Author: william.johnson@srnl.doe.gov

The burst pressure models for both thin and thick-walled PVs can be grouped into two categories, Tresca criterion-based models and von Mises criterion-based models [4], such as those included in references [2 – 8]. In general, the Tresca theory provides a lower bound prediction of burst pressure, while the von Mises theory provides an upper bound prediction of burst pressure. To determine a more accurate burst pressure solution that avoids the extremes of these theories of plasticity, Zhu and Leis [4] proposed a new theory of plasticity based on the average shear stress yield criterion predicted by both the Tresca and von Mises theories, now known as the Zhu-Leis theory [4, 9].

To augment analytical predictions of PV burst strength, Finite Element Analysis (FEA) models have often been used, particularly to model PVs with irregular geometry or damage. Built into the commercial FEA software ABAQUS, a modified RIKS model for predicting plastic instability can be used to predict PV burst strength. However, the ABAQUS RIKS model adopts the von Mises flow theory of plasticity for an isotropic material. As a result, FEA models of flawless PVs determine exactly the burst pressure that the von Mises theory predicts. Due to this, Zhu and Leis proposed a numerical technique [9] to determine, within FEA models, the more accurate Zhu-Leis burst strength, by using a critical von Mises stress criterion. Other research [10 – 12]developed FEA models for corroded pipelines. Yeom et. al. [13] compared FEA models of X70 pipeline steel to experimental data of pipes with machined defects to determine a more effective way to predict burst strength. More recently, Oh et. al. [8] obtained a large number of FEA results and used them to curve-fit an empirical equation to describe the burst pressure of PVs [8]. Phan et. al. [14] conducted similar FEA calculations but used their FEA burst pressure database to optimize parameters used in empirical theories to describe corroded pipe burst strength.

While burst models for thin-walled pressure vessels abound, work on thick-walled pressure vessels has resulted in fewer burst models [15]. Commonly used burst models include Svensson's approximate solution [16], which was derived using the von Mises flow theory to provide an upper bound estimation of burst strength, and Faupel's empirical formulae [17]. Marin [18] proposed a burst model for anisotropic thick-walled cylindrical PVs. More recently, Zheng and Lei [19] proposed a regression model for predicting burst strength based on experimental burst test data for thick-walled pressure vessels [19]. Ihn and Nguyen [20] numerically evaluated nuclear power plant pressure vessel components against these burst models and showed that the burst strength predictions from the existing burst models varied by as much as 45%, with the FEA predictions closer to the Svensson's model. This is not surprising, because both the FEA results and the Svensson model are based on the von Mises flow theory of plasticity.

Although effective, because of different theories and modeling techniques, until recently there has been no unified theory that can be used to predict both thick and thin-walled pressure vessels. In the more recent reference [8], a regression curve was developed to provide a better prediction of burst pressure for intermediate to thin-walled pressure vessels over a range of pipeline steels. Recently, Zhu et. al. [15] extended the Zhu-Leis flow theory to determine the burst strength for thick-walled PVs and showed that if the mean diameter (MD), instead of outside diameter (OD), is used for the Zhu-Leis theory for thick-walled PVs, the Zhu-Leis theory determines a burst model with similar accuracy for both thin and thick-walls. In this work the effectiveness of several different ways to measure burst strength of pressure vessels are compared. In particular, using FEA, how burst strength in thick-walled vessels is measured relative to thin-walled vessels, is

explored. The FEA burst data normalized by the thick-walled Tresca burst strength causes the burst data across the wide range of material properties studied to collapse to follow a linear relationship. A linear regression of the numerically derived burst data can predict the PV burst pressure over a wide range of material properties for both thick and thin-walled PVs. This is a first for a numerically derived burst solution and is more accurate than the commonly used Svensson solution for thick-walled pressure vessels.

2. Theoretical Models of Burst Pressure

2.1 Theoretical Models for Thin-Walled Pressure Vessels

It is commonly accepted that the burst pressure of PVs is a function of the vessel size (D/t ratio), the ultimate tensile stress (UTS) and the plastic flow response characterized by the strain hardening exponent *n* of the material. Based on the three flow theories of plasticity, i.e., the Tresca, von Mises, and average shear stress (or Zhu-Leis) theories, Zhu and Leis [4, 9] obtained a general theoretical expression for the burst pressure of thin-walled pipes or pressure vessels (D/t ≥ 20) in compact form as:

$$P_b = \left(\frac{C}{2}\right)^{n+1} \frac{4t_0}{D_{m_0}} \sigma_{uts} \tag{1}$$

where P_b is the burst pressure, t_0 is the initial wall thickness, D_{m_o} is the initial mean diameter (MD) of the pipe, n is the strain-hardening exponent, and σ_{uts} is the engineering UTS of the pipe material. The coefficient C is a yield theory dependent constant and can take on the following values:

$$C = \begin{cases} 1 & \text{Tresca Theory} \\ \dfrac{2}{\sqrt{3}} & \text{Von Mises Theory} \\ \dfrac{1}{2} + \dfrac{1}{\sqrt{3}} & \text{Zhu} - \text{Leis Theory} \end{cases} \tag{2}$$

It is apparent from Eqs. (1) and (2) that the Tresca theory provides a lower burst pressure prediction, the von Mises theory provides an upper burst pressure prediction, and the average shear stress (i.e., Zhu-Leis) theory provides an intermediate burst pressure prediction. Note that these burst pressure solutions in Eq. (1) are only applicable to thin-walled pressure vessels ($D/t \geq 20$).

For each of the three plastic flow theories, at any instantaneous loading pressure P the corresponding deformation (or the current MD and wall thickness t of the pipe) and the equivalent stress have the following relationships [9], which gives an equivalent stress versus pressure curve during loading:

$$P = \frac{1}{d}\left(\frac{C}{2}\right)^{n+1} \left(\frac{e}{n}\ln d\right)^{n} \frac{4t_0}{D_{m_0}} \sigma_{uts} \tag{3}$$

$$\sigma_{eq} = C^n \left(\frac{e}{2n}\ln d\right)^{n} \sigma_{uts} \tag{4}$$

where $d = (D_m/t)/(D_{m_0}/t_0)$, is a geometrical ratio of the current D_m/t ratio to the initial D_{m_0}/t_0 ratio for the pipe in consideration. e is Euler's number, and all other variables are as previously defined. Equation (1) defines the maximum pressure from the stress-pressure curve described by Eqs. (3) and (4).

2.2 Theoretical Models for Thick-Walled Pressure Vessels

For a thick-walled pressure vessel (D/t < 20), based on the thick shell theory, Svensson [16] in 1958 obtained the following theoretical model of burst pressure:

$$P_b = \left(\frac{0.25}{n + 0.227}\right)\left(\frac{e}{n}\right)^n \sigma_{uts} \ln\left(\frac{D_o}{D_i}\right) \tag{5}$$

where D_o is the nominal OD and D_i is the nominal inside diameter (ID). Note that this burst pressure model is not an exact solution, but an approximate solution obtained from the von Mises flow theory of plasticity that considered the UTS and the plastic flow rate of PV steels.

In order to determine burst pressure more accurately for thick-walled PVs, Zhu et. al. [15] recently developed an modified strength theory, and then extended the burst pressure model in Eq. (1) for thin-walled pipes to that for thick-walled pressure vessels as:

$$P_{zl} = 2\left(\frac{C}{2}\right)^{n+1} \sigma_{uts} \ln\left(\frac{D_o}{D_i}\right) \tag{6}$$

where C is given again by Eq. (2) and all other variables are as previously defined. The thick-wall burst pressure model in Eq. (6) can predict burst pressure for thin and thick-walled PVs.

2.3 Von Mises Failure Criterion for Determining Burst Pressure

Extensive full-scale burst tests showed that the Zhu-Leis solution in Eq. (1) determined a more accurate burst pressure for thin-walled pipes [4] than either the Tresca or the von Mises solutions. However, all commercial FEA software packages, such as ABAQUS, adopt the von Mises flow theory of plasticity, and thus determine the von Mises burst pressure solution using the RIKS model for a geometrical instability analysis. In order to use ABAQUS to determine the more accurate burst pressure, Zhu and Leis [9] developed a von Mises stress-based failure criterion by analytically determining the critical von Mises stress at the Zhu-Leis predicted burst pressure. The critical von Mises stress was determined as a function of n and UTS using a highly accurate quadratic polynomial, given as: :

$$\left(\sigma_{eq}^M\right)_c = (0.797n^2 - 0.417n + 0.932)\sigma_{uts} \tag{7}$$

where $\left(\sigma_{eq}^M\right)_c$ is the critical equivalent von Mises stress that corresponds to the Zhu-Leis burst pressure. In an FEA simulation of a PV using ABAQUS, when the von Mises equivalent stress reaches the $\left(\sigma_{eq}^M\right)_c$ value for the PV material, the burst failure occurs, and the corresponding pressure is the FEA determined burst pressure of the PV.

2.4 Limit Load Criteria for Determining Burst Pressure

In practice, the limit load criteria are often used to determine burst failure for any PV in the loading conditions of pure pressure or combined loading. Three commonly used limit load criteria applied to pressure versus strain curves of PVs are the twice elastic slope, the zero slope, and the tangent intersection criteria. These three criteria and their relative predicted values are illustrated in Fig. 1. The twice elastic criterion calculates the burst pressure as the intercept value on the pressure-strain curve where it intersects a line with twice the elastic slope [8]. The tangent intercept criterion calculates the burst pressure as the pressure value when the tangent line, recommended at 5% strain, intercepts a tangent line to the elastic portion of the curve [21]. The zero-slope criterion calculates the burst pressure as the pressure where the pressure-strain curve reaches a maximum [22]. In terms of relative comparison, the twice-elastic criterion tends to calculate the lowest burst pressure, the tangent intersection criterion an intermediate burst pressure, and the zero-slope criterion the highest burst pressure value.

In comparison to the three limit load criteria just discussed above, the three plastic theoretical models in Eq. (1) may provide comparable predictions to the limit load predictions shown in Fig. 1. As a matter of fact, because these burst pressure values were derived by enforcing the plastic instability condition of $\partial P/\partial \epsilon = 0$, the von Mises burst pressure prediction provides an identical prediction to the zero-slope limit load criterion prediction.

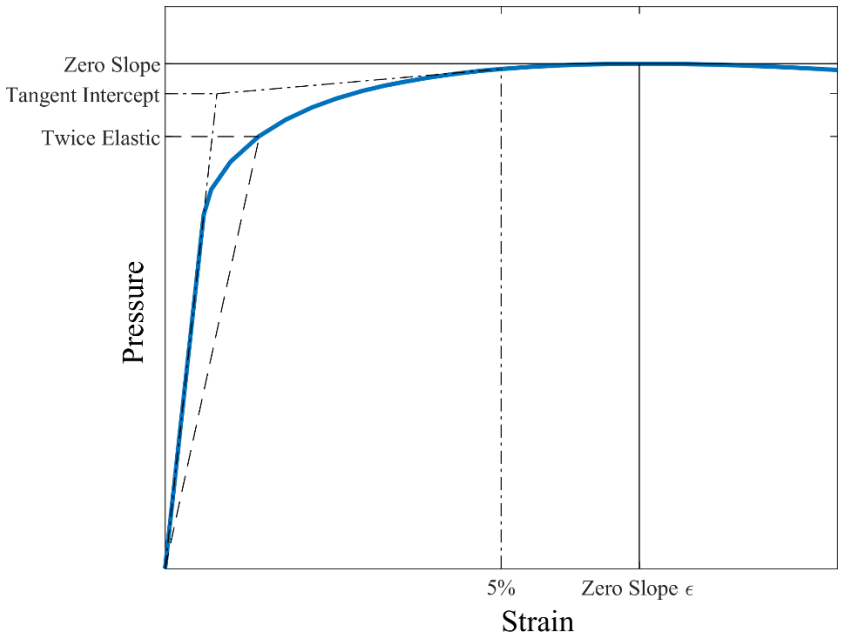

Figure 1. Illustration of the zero-slope, tangent-intercept, and twice elastic limit load criteria from the pressure-strain curve for a pressure vessel or pipe.

3. Finite Element Models

This work employed the FEA commercial software package ABAQUS for all FEA simulations and the parametric study of burst strength for PVs with various geometries and steel grades. Material and geometric nonlinearities were considered in all FEA models. In particular, the elastic-plastic isotropic hardening model that obeys the von Mise flow theory of plasticity was adopted within the large deformation framework for all models. Further detail on the FEA models is provided below.

3.1 Material and Analysis Assumptions

For this study, it is assumed that the material follows a power-law strain hardening rule. For a power-law hardening material, the FEA models utilized material input data from the following true stress-strain curve:

$$\sigma = \begin{cases} E\varepsilon, & \sigma < \sigma_{ys} \\ K\varepsilon^n, & x \geq \sigma_{ys} \end{cases} \tag{8}$$

where

$$K = \left(\frac{e}{n}\right)^n \sigma_{uts}. \tag{9}$$

In Eqs. (8) and (9) σ is the true stress and ε is the logarithmic strain determined in a uniaxial tensile test. E is the Young's modulus, σ_{ys} is the yield strength, K is the strength coefficient, and n is the strain hardening exponent of the material. This research investigates the burst strength of thin and thick-wall cylindrical pressure vessels for the pipeline steels of Grade B, X52, X65, X70, and X80, covering low to high pipeline grades which are frequently used in the oil and gas industry. Table 1 lists the material properties for each of the pipeline steels used in the FEA models, where the yield and ultimate tensil strengths meet the minimum specified properties by API 5L [23].

Table 1. Material properties for pipeline steels used in the FE models.

	E (psi)	ν	σ_{ys} (ksi)	σ_{uts} (ksi)	n
Grade B	30e6	0.3	35.5	60.2	0.192
X52	30e6	0.3	52.2	66.7	0.111
X65	30e6	0.3	65.3	77.6	0.089
X70	30e6	0.3	70.3	82.7	0.085
X80	30e6	0.3	80.5	90.6	0.068

With the input material property data of the stress-strain curve in the format of Eq. (8), the elastic-plastic FEA simulations are performed using ABAQUS for a specific cylindrical vessel subjected to internal pressure. Using the RIKS model, ABAQUS provides the load-displacement path for the PV, from which the von Mises flow theory based burst strength at the geometric instability, i.e. plastic collapse, can be determined. On the other hand, from the numerical relationship of the von Mises equivalent stress versus internal pressure and using the critical von Mises stress in Eq. (7), the FEA Zhu-Leis burst pressure is determined. Alternatively, from the

numerical relationship of the hoop strain versus internal pressure and using the three limit load criteria discussed in Section 2.4, the failure pressure can be determined for each limit load criterion.

3.2 Model Meshing and Convergence

An example mesh for the FE plane strain model is shown in Fig. 2. Because this work examined a variety of different geometric conditions, the mesh size between models was not consistent. However, the models were meshed to maintain an approximately square aspect ratio, and all were modeled with 5 elements through the thickness. Figure 3 shows the results of a mesh sensitivity study. The results show that by 3 elements through the thickness the mesh had converged. Therefore, the 5 elements used through the thickness for higher resolution of the stress-strain field, is more than sufficient to accurately capture the PV burst pressure.

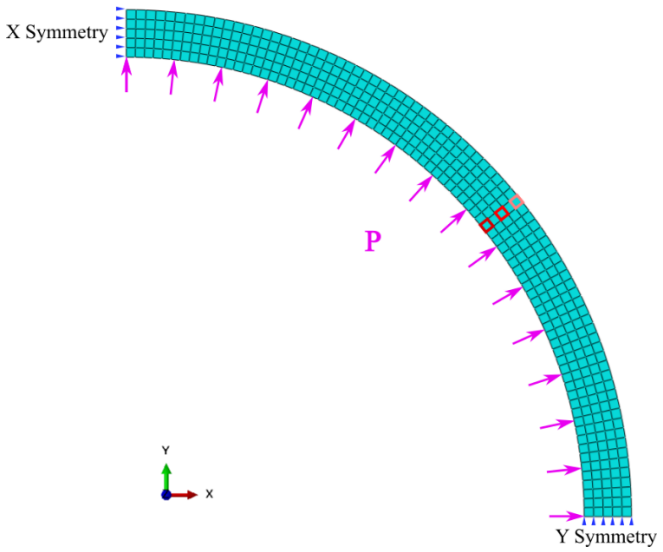

Figure 2. FE plane strain PV geometry, mesh, boundary conditions, and loading, with measurement locations at the ID, MD, and OD highlighted in dark red, red, and pink, respectively for $D_o/t_o = 21.3$.

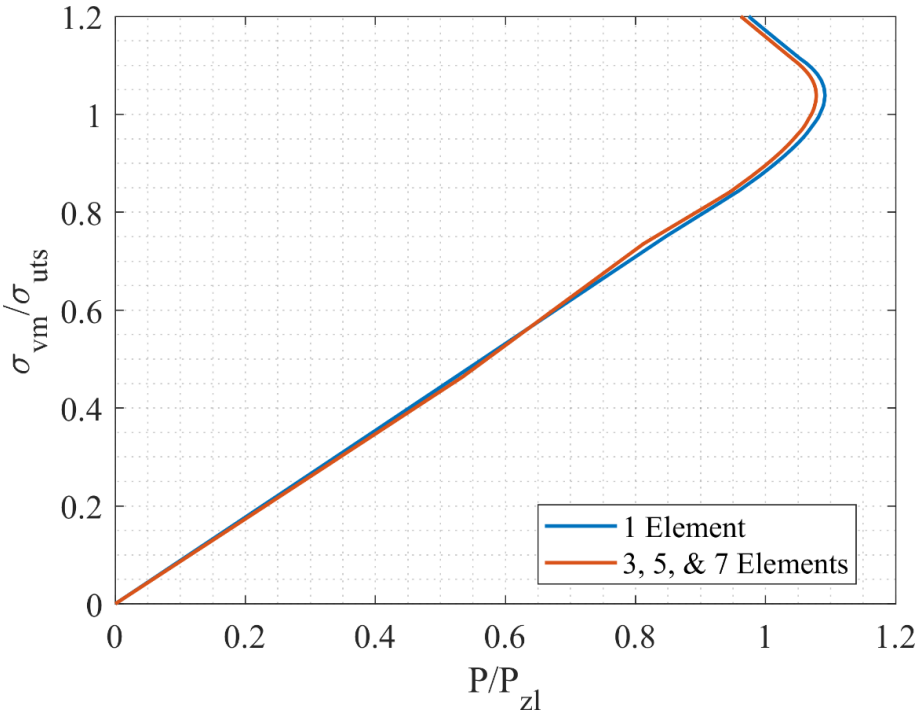

Figure 3. Pressure-stress curves from the mesh sensitivity study show that meshes with 3 or more elements through the thickness provide identical pressure-stress curves, confirming that the mesh is converged for the 5 element through thickness case used in this study.

3.2 Comparison of 2D vs 3D FEA Models

Generally, an end-capped PV is analyzed using a 3D FEA model with solid elements (e.g. 8-noded bricks) to consider the end effect or local deformation if the PV has a defect. For a long, defect-free pipe subject to internal pressure, as considered in this work, a 2D plane-strain model should be sufficient. To verify this, a $1/8^{th}$ pipe 3D model was created and compared to a quarter pipe 2D plane-strain model. The geometry, mesh, boundary conditions, and loading are shown for the 2D and 3D plane strain FEA models respectively, in Figs. 2 and 4. Both have x and y-symmetry boundary conditions applied on the y and x surfaces respectively, to account for the symmetry in the x and y directions. The 3D model also has a z-symmetry boundary condition applied at the mid plane ($z = 0$), and the remote end is fixed to simulate a capped constraint condition, where $z = -L/2$. $L = 12D$ is the total pipe length used in the FEA 3D simulation. Internal pressure is applied on the inside of the pipe for both 2D and 3D FEA models.

Figure 5 shows a comparison of the results for the 3D and 2D plane strain model at the mean diameter. The difference between the maximum pressure for the two models is less than 0.1%, which for practical purposes indicates that the 2D and 3D FEA models are nearly identical to each other for simulating a long, defect-free or end capped pipe. Thus, for all further FEA simulations, the 2D plane strain FEA model is used to significantly decrease computation time.

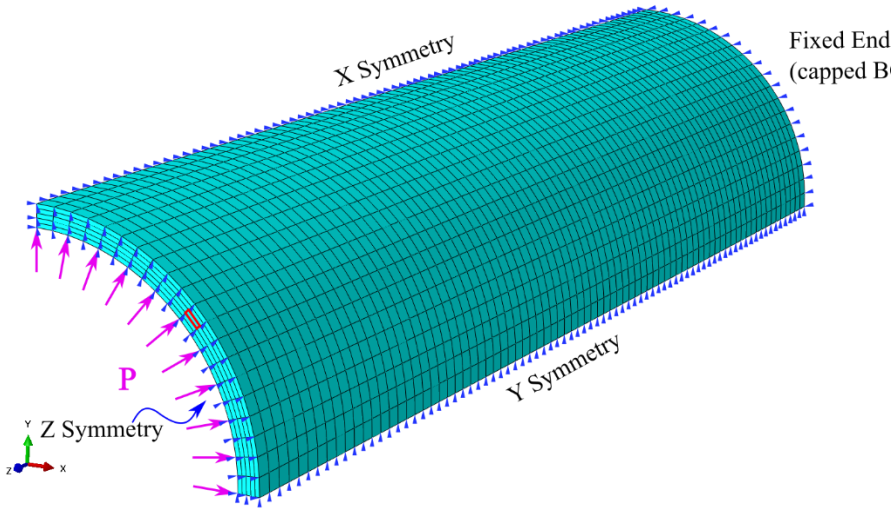

Figure 4. FEA 3D PV geometry, mesh, boundary conditions, and loading, with measurement location at the MD highlighted in red for $D_o/t_o = 21.3$.

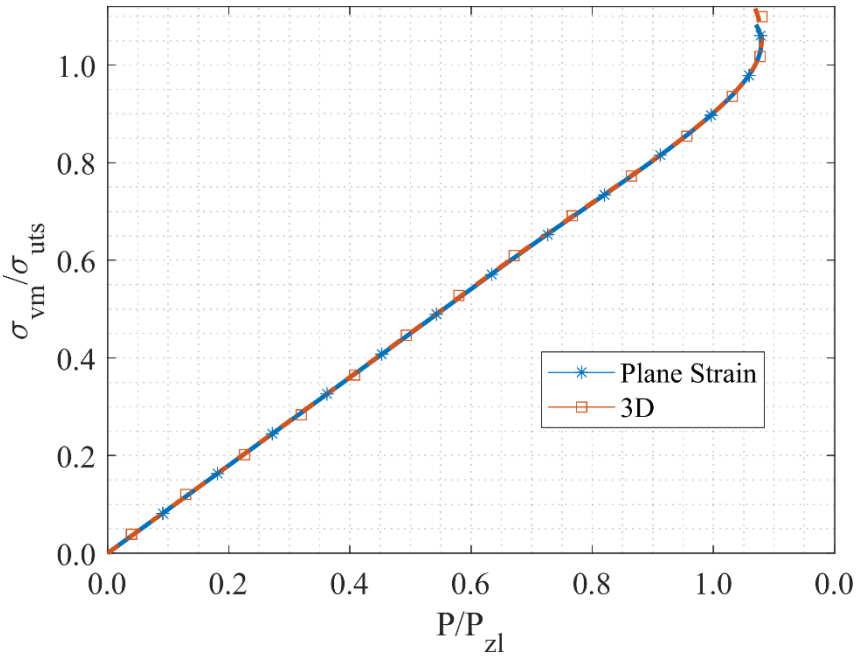

Figure 5. Comparison of 3D and plane strain FEA model pressure-stress (von Mises) burst curves, with stress normalized by the UTS and pressure normalized by the Zhu-Leis burst pressure in Eq. (5).

3.3 Comparison of Failure Criteria

A comparison of the failure criteria discussed in Section 2 is performed in this section on two different pipe geometries: a thick-walled pipe with $D_o/t_o = 10.7$ and an intermediate-walled pipe with $D_o/t_o = 21.3$. Figure 6 shows the evaluation of the limit load criteria from the FEA

results for the $D_o/t_o = 10.7$ case, while Fig. 7 shows a comparison of the FEA response to the predicted analytical responses and burst pressures using Eqs. (3) – (6). From the FEA results of the $D_o/t_o = 21.3$ intermediate-wall case, Fig. 8 shows the limit load criteria predicted burst pressures, and Fig. 9 shows the analytical responses and burst pressures. The pressure-stress relationship, in Figs. 7 and 9, is usually presented with the pressure along the abscissa and stress along the ordinate axes, as shown in Fig. 5. This is because within the PV the stress is a function of the pressure. However, to provide for ease of comparison between the analytically predicted responses and the limit load responses, which are usually plotted with pressure along the ordinate axis, Figs. 7 and 9 measure the stress along the abscissa and the pressure along the ordinate axis. In Figs. 3 and 5 – 9 the burst pressure is normalized by P_{zl}. This is to emphasize how the various burst pressure techniques compare to the Zhu-Leis burst pressure.

Table 2 lists the predicted burst pressures for the six different techniques. The predicted values show that the twice elastic and Tresca analytical predictions for both cases are similar, with the Tresca theory predicting a burst pressure approximately 2.5% lower than the twice elastic criterion. The Zhu-Leis theory predicted an intermediate value approximately 8% higher than the Tresca theory value. The tangent intersection criterion did not provide a prediction because the zero-slope point on the curve occurred before 5% strain. The von Mises theory and zero-slope limit load criterion provided identical predictions of burst pressure.

These comparisons demonstrate some problems with the limit load criteria. The twice elastic slope criterion is somewhat arbitrary. The predicted burst strength could vary in how conservative it is based on the strain hardening of the material. The tangent intersection criterion is ambiguous. Although 5% strain is the recommended evaluation point for the tangent, if the pressure-strain curve reaches a maximum before this, it either reduces to the zero-slope criterion or else the slope needs to be evaluated at an arbitrarily chosen strain less than the zero-slope strain. In this case the tangent-intersection criterion could be evaluated at a strain that provides a burst pressure in the range from the pressure at yielding onset to the zero-slope pressure. The zero-slope pressure prediction has the same drawbacks as the von Mises theory prediction. It provides an upper bound which tends to overpredict the burst pressure. The strength of the Zhu-Leis theory is that it provides an unambiguous intermediate burst pressure value which is not overly conservative and has been shown in other studies (e.g., references[2, 7, 24]) to accurately predict the burst pressure when compared to full-scale experimental burst data.

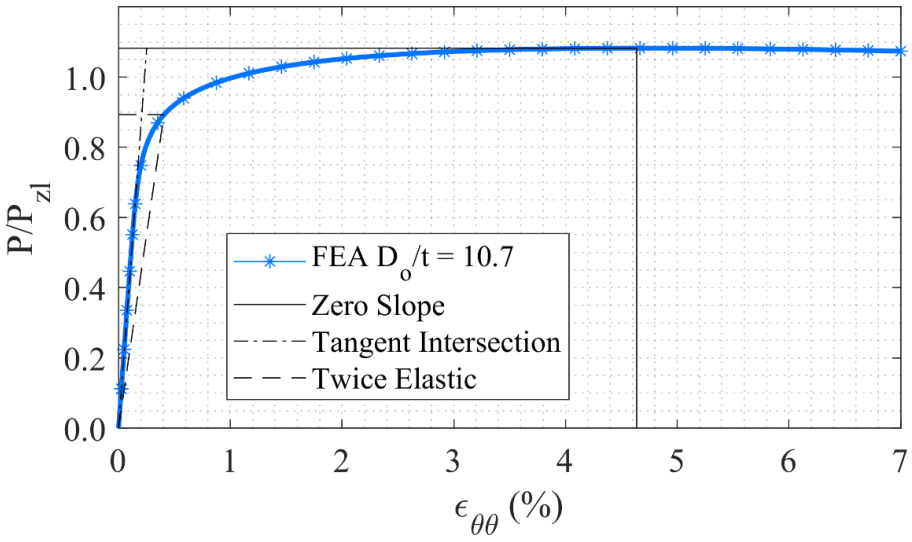

Figure 6. Comparison of limit load criteria burst predictions for $D_o/\mathrm{t_o} = 10.7$ FEA model.

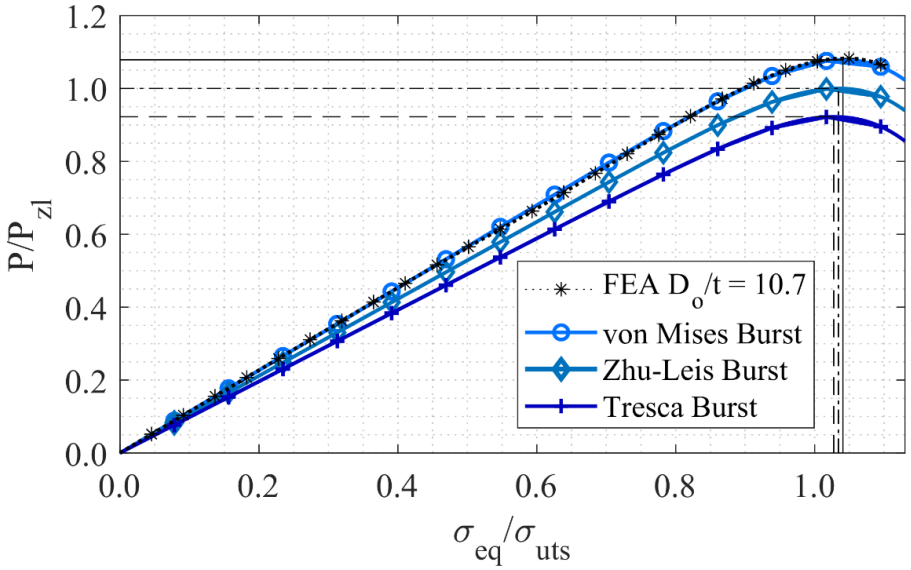

Figure 7. Comparison of analytical solution burst predictions for $D_o/\mathrm{t_o} = 10.7$ FEA model.

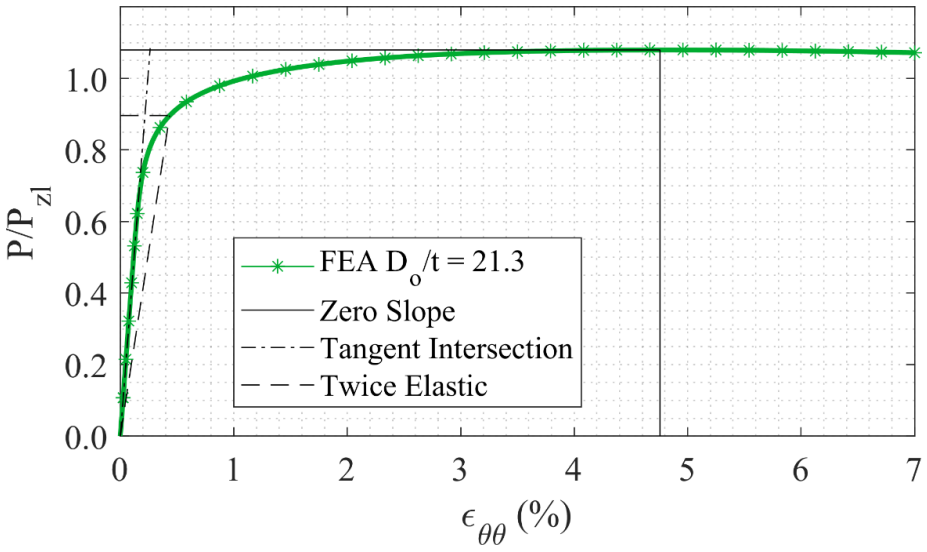

Figure 8. Comparison of limit load criteria burst predictions for $D_o/\mathrm{t_o} = 21.3$ FEA model.

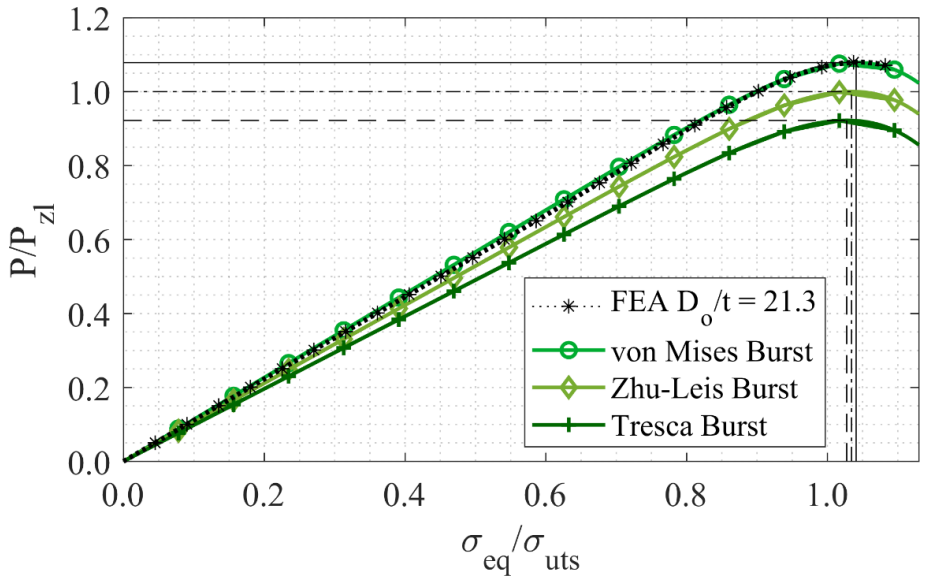

Figure 9. Comparison of analytical solution burst predictions for $D_o/t_o = 21.3$ FEA model.

Table 2. Comparison of the burst pressures (in ksi) predicted by the different limit load techniques (gray columns) and comparable theories for an intermediate and thick-walled PV.

	Twice Elastic	Tresca	Tangent Intersection	Zhu-Leis	Zero Slope	Von Mises
$D_o/t = 10.7$	15.5	15.1	NA	16.4	17.7	17.7
$D_o/t_o = 21.3$	7.4	7.2	NA	7.8	8.4	8.4

3.4 Thick Wall Effect on FEA Simulations

The critical von Mises stress in Eq. (7), corresponding to the Zhu-Leis burst pressure, was derived for thin-wall shell theory. In the derivation, the hoop stress was assumed to be uniformly distributed through the thickness. However, this assumption does not hold for thick-walled PVs. Figures 10 and 11 compare the von Mises stress at the ID, MD, and OD for $D_o/t_o = 21.3$ and $D_o/t_o = 10.7$, respectively. These figures show that for the "thin-walled" pipe with $D_o/t_o = 21.3$, the pressure-stress curves show a small amount of variation over the entire loading curve. However, for the thick-walled pipe with $D_o/t_o = 10.7$, the variation is much larger during the elastic loading. As plastic yielding occurs, the three stress-pressure curves at ID, MD, and OD converge.

Table ***3*** compares the predicted critical stress using Eq. (7) with the graphically determined critical stress from Figs. 10 and 11 for the ID, MD, and OD stress measurement locations. For the $D_o/t_o = 21.3$ case, the difference between the stress at the three diameters and the critical point stress are all less than 1%, suggesting that the location of stress measurement will introduce little error. However, for the $D_o/t_o = 10.7$ case the error between the predicted critical stress and the ID and OD are 1.4% and 2.3% respectively. The MD predicted stress was only 0.5% different from the critical point stress. These results suggest that the Zhu-Leis burst pressure can be predicted numerically for thick-walled PVs using Eq. (7), which was derived for thin-walled PVs, as long as the von Mises stress is measured at the MD of the PV in the FEA model. Due to this result, for all further models in this study, the von Mises stress was measured at the MD.

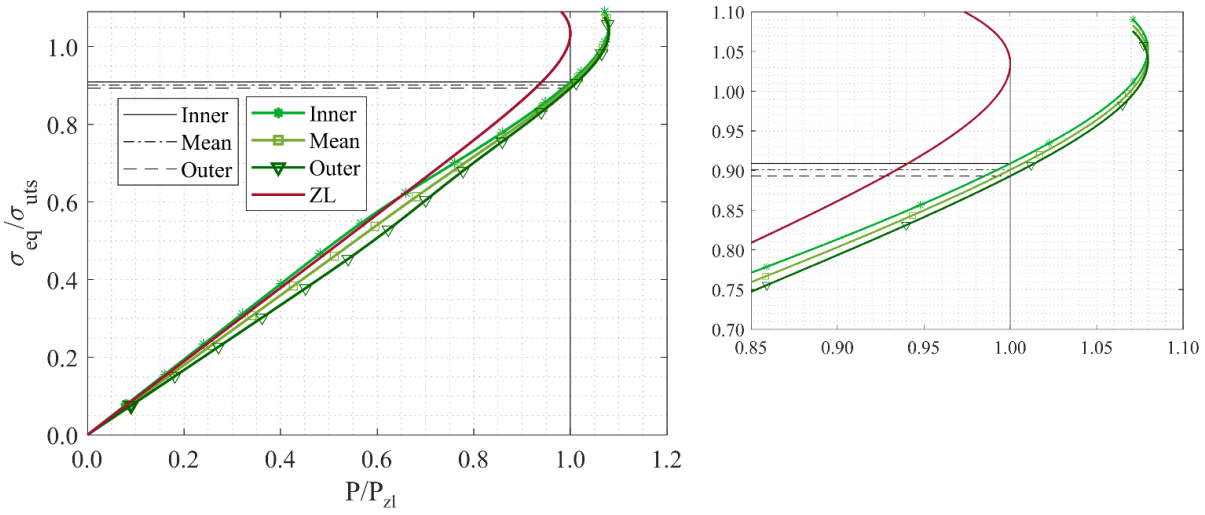

Figure 10. Comparison of $D_o/t_o = 21.3$ FEA calculated stress at the ID, MD, and OD as described in Fig. 2, showing where the curves intersect (the critical point given by Eq. (7)) the analytical Zhu-Leis (ZL) average shear stress predicted pressure-stress curve (black dashed and solid lines), with detailed view.

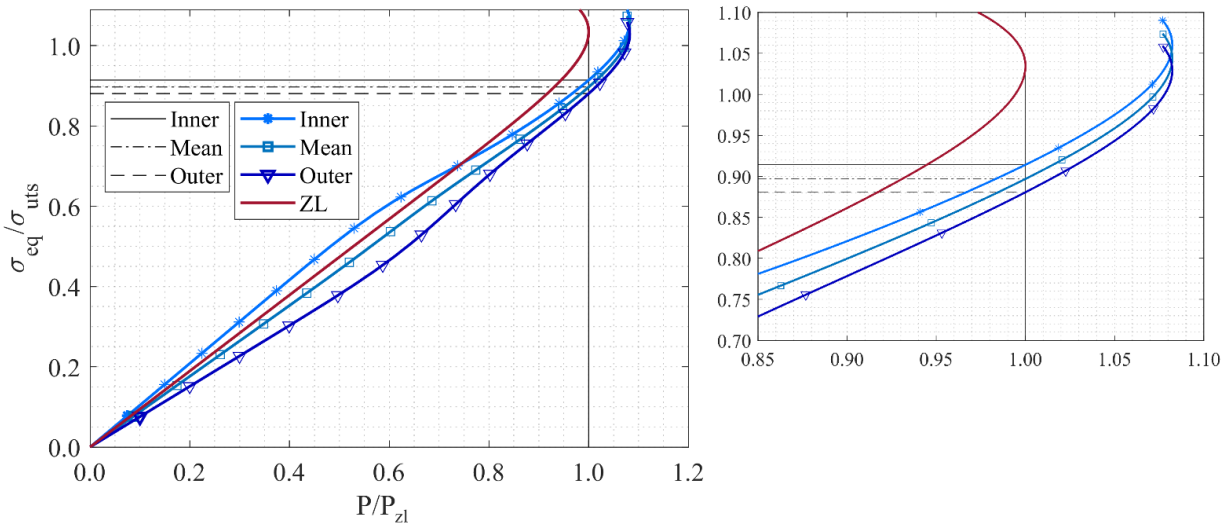

Figure 11. Comparison of $D_o/t_o = 10.7$ FEA calculated stress at the ID, MD, and OD as described in Fig. 2, showing where the curves intersect (the critical point given by Eq. (7)) the analytical Zhu-Leis predicted pressure-stress curve (black dashed and solid lines), with detailed view.

Table 3. Comparison of the von Mises stresses at the ID, MD, and OD of the PV as compared to the predicted critical point stress (Eq. (7)) for the ZL theory predicted burst pressure.

	$(\sigma_{eq}^{M})_c$ (ksi)	ID (ksi)	% Diff.	MD (ksi)	% Diff.	OD (ksi)	% Diff.
$D_o/t = 10.7$	69.93	70.94	1.4	69.60	0.5	68.34	2.3
$D_o/t_o = 21.3$	69.93	70.53	0.9	69.91	0.03	69.31	0.9

4. Numerical Determination of Burst Strength

4.1 Parametric Finite Element Study

Under the conditions described in Section 3, a fully parametrized study was conducted on 12 different common PV geometries, described in

Table ***4***, ranging from $D_o/t = 8$ to $D_o/t = 120$, each evaluated using the five pipeline steels described in Table 1, for a total of 60 different FEA model cases. The ABAQUS Python capability greatly facilitated this parametric study. It has the ability to rapidly iterate over multiple models (e.g. reference [25]) by generating all aspects of the model, from geometry creation to job submission, using Python scripting commands.

Figure 12 shows a diagram and flow chart of the Python and MATLAB codes used for the parametric FEA models. The code used as initial inputs the materials and geometry provided in Tables 1 and 4, respectively. For each combination of materials and D/t ratios it would:

1. Generate the geometry (example shown in Fig. 2) and materials.

2. Make material section assignments, generate the FEA mesh, and create the analysis step.
3. Create the assembly, boundary conditions and loads, the chosen element sets at the MD for monitoring the pressure and stress consistent with the findings in Section 3.3 (example also shown in Fig. 2), and history output requests for those element sets.
4. Run the model and extract the pressure and stress data from the output file. It would then save this data to a text file.
5. Repeat steps 1 – 4 for the next combination of materials and geometry until all material models and geometry were completed.

Once the models and FEA calculations finished, a separate MATLAB script further post-processed the data. Although this could have been accomplished in Python, because of the limited Python plotting capabilities within the ABAQUS Python API, MATLAB made it much easier to visualize and check that the algorithm was processing the data correctly. Once the data was handed off to the MATLAB algorithm, it performed the following analyses:

1. Imported the data from a text file for a specific material-geometry pair and plotted the pressure-stress curves.
2. Calculated both the von Mises and Zhu-Leis theory burst pressures. These could easily be checked visually (e.g. the code generated figures similar to Figs. 10 and 11) against the predictions to ensure the algorithm was finding the correct burst pressure in the data.
3. Added the material and geometric parameters, and numerically predicted burst pressures to the burst pressure database.
4. Repeated steps 1 – 3 for each combination of materials and geometry.

The final output to the Python and MATLAB scripts was a database containing the numerically predicted von Mises and Zhu-Leis burst strengths for 60 different PV material and geometric configurations that are common in the pipeline industry. Once the code was written the entire runtime for the simulations and extracting the data took approximately 2 hours. This technique could very easily be used to quickly generate much larger databases or very rapidly analyze a specific case of interest. This study only used 60 different models because they adequately spanned both the design and material space of interest.

Table 4. Geometries used in the PV parametric study.

Case No.	Diameter (in)	Thickness (in)	D_o/t_o
1	8	1	8
2	8	0.75	10.7
3	8	0.5	16
4	16	0.75	21.3
5	16	0.5	32
6	24	1	24
7	24	0.5	48
8	24	0.25	96
9	30	0.75	40

10	30	0.5	60
11	30	0.25	120
12	42	0.5	84

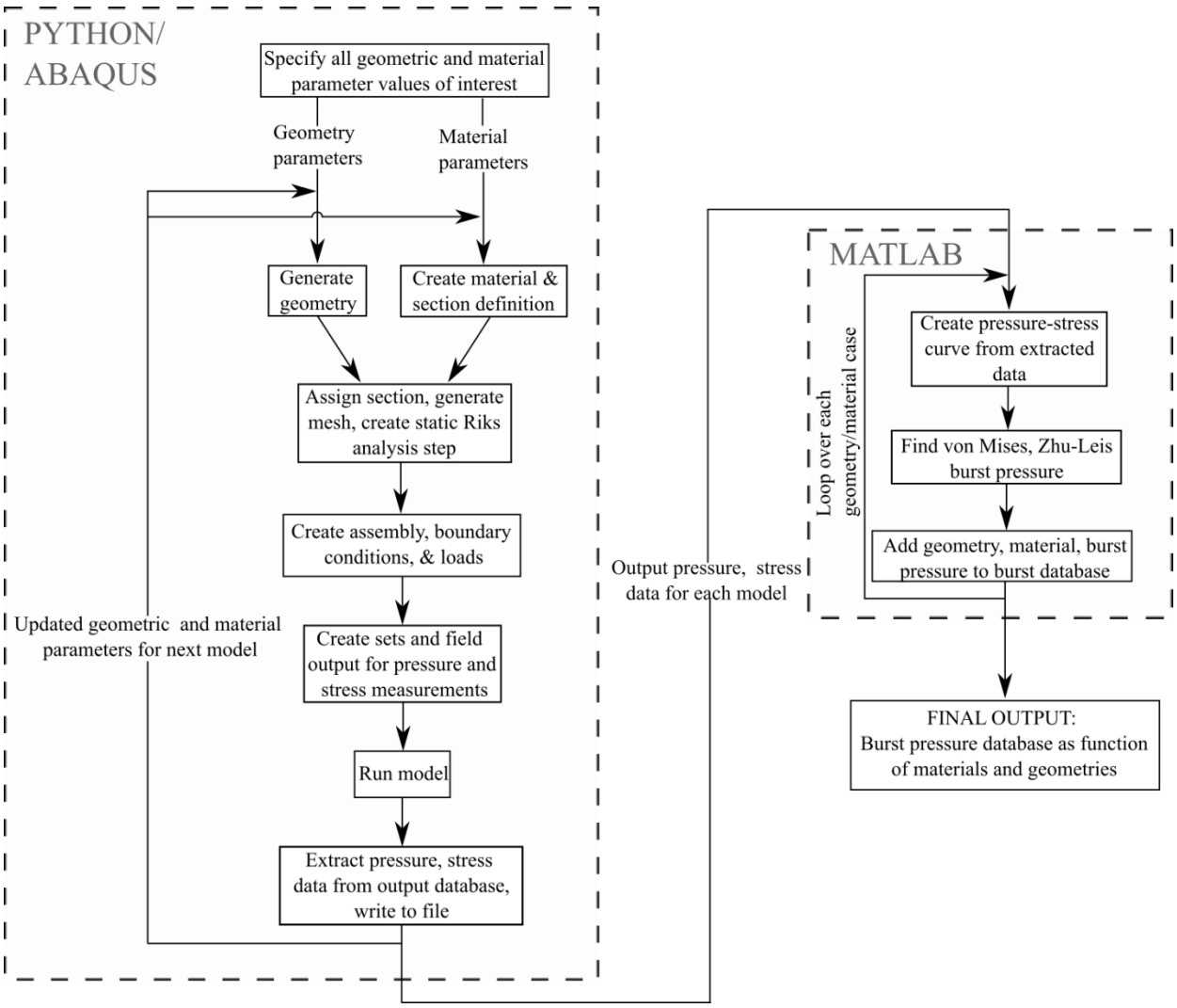

Figure 12. Diagram of Python and MATLAB code flow to generate Abaqus FE models, extract data, and create a burst pressure database as a function of materials and geometries.

4.2. Regression Analysis of FEA Results

The above parametric FEA study has determined 60 burst pressure data as a function of D/t, UTS, and n. An FEA model of burst pressure could be developed by the curve-fit or regression approach. However, a three-variable regression is very difficult to perform if not impossible in some cases. Generally, a data normalization approach is first applied to reduce the regression variables. Development of the Zhu-Leis criteria in previous research normalized burst pressure data by the thin walled Tresca strength solution, which is a function of n only [9]. In this work the burst pressure is normalized by the thick-wall Tresca strength solution originally provided by

Turner [26], $P_T = \sigma_{uts} \ln (D_o/D_i)$, as shown in Fig. 13, where the normalized FEA burst strength is plotted as a function of n. In this figure the burst strength was determined by using the critical von Mises equivalent stress criterion in Eq. (7) and the FEA results of the von Mises stress extracted from the parametric study in Section 4. The results, when normalized by the thick-wall Tresca strength solution, show that the normalized burst strength reduces to an approximately linear function of the single variable *n* with very small scatter.

Linear regression method was used to determine the following relationship between normalized burst pressure $\hat{p}$ and n:

$$\hat{p}(n) = 1.079 - 0.6395n \tag{10}$$

where

$$\hat{p} = \frac{P_b}{\sigma_{uts} \ln\left(\frac{D_o}{D_i}\right)}. \tag{11}$$

From the normalized expressions in Eqs. (10) and (11), burst pressure is written as a function of D_o/D_i, UTS, and n:

$$P_b(n, \sigma_{uts}, D_o, D_i) = (1.079 - 0.6395n)\sigma_{uts} \ln\left(\frac{D_o}{D_i}\right) \tag{12}$$

The normalized FEA data of burst pressure, as shown in Fig. 13, fall within the yellow bounding envelope. The data varies from $\hat{p}(n)$ by less than 0.5% regardless of material or geometric dimensions. Because there is so little error between the curve fit and the FEA data, this linear curve can be used to predict the burst pressure for both thin and thick-walled PVs for materials ranging from Grade B to X80 pipeline steels.

In contrast to Fig. 13, Fig. 14 shows the same parametric study data normalized by the Tresca strength solution $P_T = \sigma_{uts} 2t_0/D_o$ for thin-walled pipes from reference [4]. In this case, the normalized burst strength is a function of *n* and the D_o/t_o ratios, resulting in a very large scatter. This implies that the load normalization using the thin-wall Tresca burst solution may be inappropriate and should be avoided for use with thick-walled PVs.

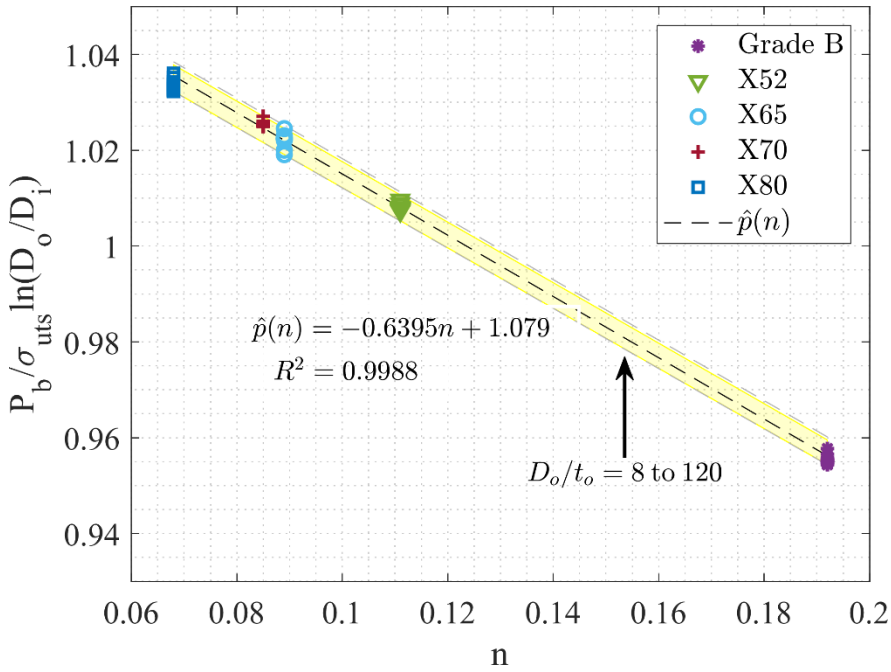

Figure 13. Burst pressure normalized by the thick-wall Tresca solution for all 60 data points from the parametric study, along with a linear interpolation $\hat{p}(n)$ and bounding envelope (dashed gray lines).

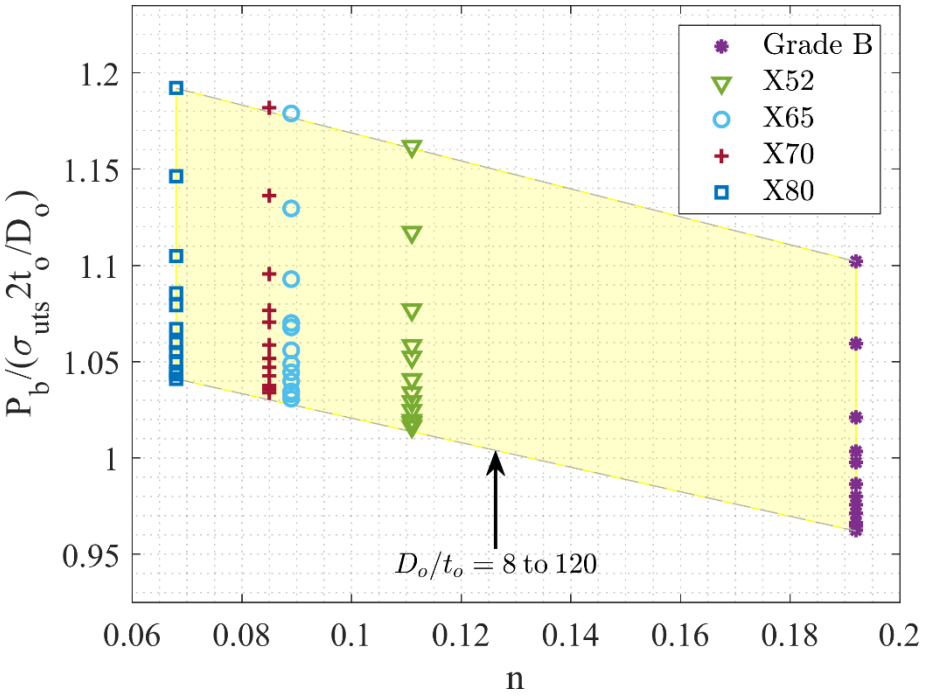

Figure 14. Burst pressure normalized by the thin-wall solution normalization for all 60 data points from the parametric study.

5. Validation of Proposed Burst Strength Model

5.1. Comparison of Proposed Model Predictions with FEA Results

To assess the goodness of fit of the proposed model in Eq. (10), the model predictions are compared with the raw FEA results of burst strength for the lower Grade B steel, intermediate grade X52 and high grade X80, as shown in Table A1 of the appendix. These materials were chosen for validation because they span the range of materials of interest. Note that the FEA burst pressure data are the approximate results of the Zhu-Leis burst pressure. Also included in Table A1 is the burst pressure predicted using the Svensson model in Eq. (5), which is currently the most commonly used model to predict thick-walled PV burst strength, hence its inclusion for comparison to the proposed model herein. The percent error from the FEA burst pressure was also included.

The results show that the proposed burst model has less than 1% error from the FEA burst data for all materials and geometries examined. The Svensson burst model consistently overpredicts the burst pressure by ~ 4% for Grade B and by ~ 6% for X80. Error for both models grew as the wall thickness increased by approximately the same amount. The Svensson model overpredicts burst strength because it is based on the von Mises flow theory of plasticity. The high accuracy of the proposed burst model in Eq. (10) confirms that it accurately captures the material – geometry – burst pressure relationships.

5.2. Comparison of Proposed Model to Full-Scale Burst Data

For further validation, Fig. 15 compares the proposed model in Eq. (10) to full scale burst data provided by a variety of references in the literature ([27 – 38]) over a wide range of strain hardening exponent values and geometries ranging from thin ($D/t = 114$) to thick ($D/t = 6$) walled PVs. The burst pressure data for thick-walled PVs are indicated by filled in markers. Figure 15, which is a recreation of Fig. 6 in reference [4], but using the thick-wall normalization, shows that the proposed model matches very closely to the analytically developed Zhu-Leis burst pressure solution, and provides a mean between the upper bounding von Mises and lower bounding Tresca based burst solutions. These results provide confidence that the proposed model supplies accurate predictions of the burst pressure of PVs over a wide range of both materials and geometries.

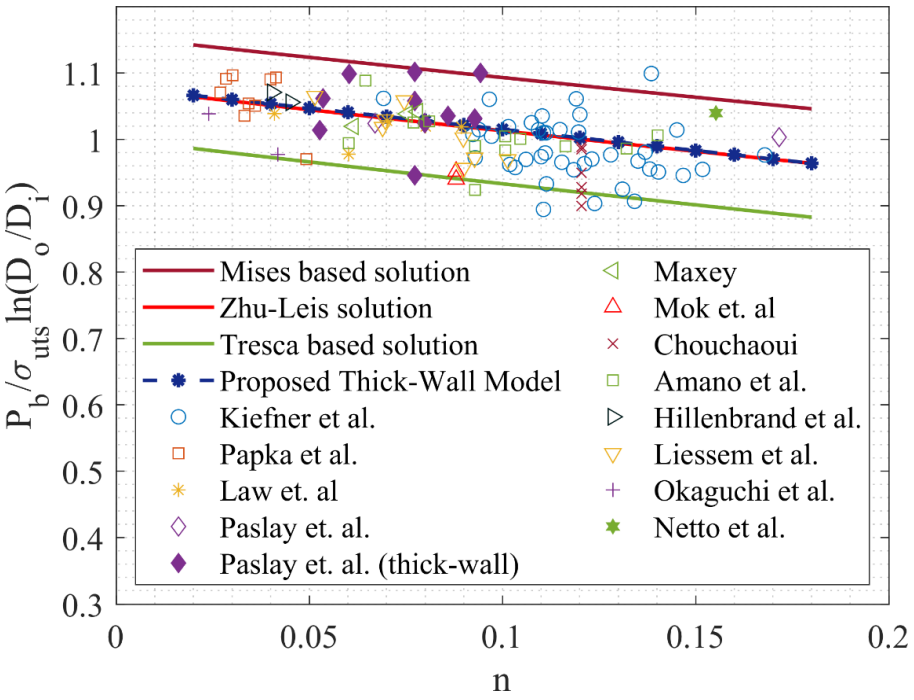

Figure 15. Comparison of the proposed model to full-scale reference data, as well as the theories described in Eqs. (2) & (5).

6. Conclusions

This paper performed a parametric FEA study for a wide range of thin and thick-walled PVs and presented a new burst pressure model for the prediction of pressure vessel burst strength. This model can predict the burst strength for both thick and thin-walled PVs over a wide range of line pipe steels. The primary results include:

1) A confirmation that 2D plane strain models accurately captured the burst pressure when compared to full 3D models, thus allowing for much simpler FEA models and very rapid FEA model run time.
2) Direct comparisons of the common limit load criteria to a critical Mises stress criterion demonstrating the limitations of limit load criteria and highlighting the advantages of the analytical models.
3) Evaluation of the PV wall thickness effect showed that the mean diameter was a more accurate diameter parameter to measure the stresses and strains in the PV to predict burst strength for both the thin and thick-walled PVs.
4) FEA databases of burst pressure can be rapidly built using ABAQUS Python scripts for a variety of materials and geometries, using the coding framework presented in this work.
5) The numerical and experimental validations showed that the proposed burst pressure model is much simpler than the Svensson model, and can accurately predict burst pressure for thin and thick-walled PVs over a wide range of line pipe steels and typical geometries.

The work presented here was developed over a range of pipeline steels from Grade B to X80, (all carbon steels) and follow the power-law hardening rule. Thus the FEA burst model developed in this work is applicale to carbon steels, alloy steels, stainless steels, ductile composites or other materials that obey the power-law strain hardening relationship, but not applicable to non-power-law materials. This work was developed over range of geometries with D/t ratios ranging from 8 to 120. This is a very wide range of D/t ratios. Outside of this range the results, such as Eq. (12), may still be valid, but should be verified with additional analysis.

Acknowledgements

This work was supported by the Laboratory Directed Research and Development (LDRD) program within the Savannah River National Laboratory (SRNL). This document was prepared in conjunction with work accomplished under Contract No. 89303321CEM000080 with the U.S. Department of Energy (DOE) Office of Environmental Management (EM).

References

[1] J. Spence and D. H. Nash, "Milestones in pressure vessel technology," *International Journal of Pressure Vessels and Piping,* Vol. 81, pp. 89-118, 2004.

[2] M. Law and G. Bowie, "Prediction of failure strain and burst pressure in high yield-to-tensile strength ratio linepipe," *International Journal of Pressure Vessels and Piping,* Vol. 84, pp. 487-492, 2007.

[3] T. Cristopher, B. Rama Sarma, P. Govindan Potti, B. Nageswara Rao and K. Sankarnarayanasamy, "A comparative study on failure of pressure estimations of unflawed cylindrical vessels," *International Journal of Pressure Vessels and Piping,*Vol. 79, pp. 53 - 66, 2002.

[4] X.-K. Zhu and B. N. Leis, "Average shear stress yield criterion and its application to plastic collapse analysis of pipelines," *International Journal of Pressure Vessels and Piping,* Vol. 83, pp. 663-671, 2006.

[5] DNV, Offshore Standard DNV-OS-F101, Det Norske Veritas, Norway, 2013.

[6] G. Stewart, F. Klever and D. Ritchie, "An analytical model to predict the burst capacity of pipelines," in *13th International Conference on Offshore Mechanics and Arctic Engineering*, Houston, TX, 1994.

[7] X.-K. Zhu and B. N. Leis, "Evaluation of burst pressure prediction models for line pipes," *International Journal of Pressure Vessels and Piping,* Vol. 89, pp. 85-97, 2012.

[8] D. H. Oh, J. Race, S. Oterkus and E. Chang, "A new methodology for the prediction of burst pressure for API 5L X grade flawless pipelines," *Ocean Engineering,* Vol. 212, p. 107602, 2020.

[9] X.-K. Zhu and B. N. Leis, "Theoretical and numerical predictions of burst pressure of pipelines," *Journal of Pressure Vessel Technology,* Vol. 129, pp. 644-652, 2007.

[10] A. Karstensen, A. Smith and S. Smith, "Corrosion damage assessment and burst test validation of 8in X52 linepipe," in *Proceedings of ASME Pressure Vessel and Piping Conference*, Atlanta, GA, 2001.

[11] B. Fu and M. Kirkwood, "Determination of failure pressure of corroded linepipes using the nonlinear finite element method," in *Proceedings of the Second International Pipeline Technology Conference, Vol. II*, Ostend, Belgium, 1995.

[12] J. B. Choi, B. K. Goo, J. C. Kim, Y. J. Kim and W. S. Kim, "Development of limit load solutions for corroded gas piplines," *International Journal of Pressure Vessels and Piping,* Vol. 80, pp. 121 - 128, 2003.

[13] K. J. Yeom, Y.-K. Lee, K. H. Oh and W. S. Kim, "Integrity assessment of a corroded API X70 pipe with a single defect by burst pressure analysis," *Engineering Failure Analysis,* Vol. 57, pp. 553-561, 2015.

[14] H. C. Phan, A. S. Dhar and B. C. Mondal, "Revisiting burst pressure models for corroded pipelines," *Canadian Journal of Civil Engineering,* Vol. 44, no. 7, pp. 485-494, 2017.

[15] X.-K. Zhu, B. Wiersma, R. Sindelar and W. R. Johnson, "New strength theory and its application to determine burst pressure of thick-wall pressure vessels," in *Proceedings of the ASME 2022 Pressure Vessels & Piping Conference*, Las Vegas, NV, 2022.

[16] N. L. Svensson, "The bursting pressure of cylindrical and spherical vessels," *Journal of Applied Mechanics,* Vol. 25, pp. 89-96, 1958.

[17] J. H. Faupel, "Yield and bursting characteristics of heavy-wall cylinders," *Transactions of the American Society of Mechanical Engineers,* Vol. 78, no. 5, pp. 1031 - 1061, 1956.

[18] J. Marin and T. L. Weng, "Strength of thick-walled cylindrical pressure vessels," *Journal of Manufacturing Science and Engineering,* Vol. 85, pp. 405-415, 1963.

[19] C. X. Zheng and S. H. Lei, "Research on bursting formula of mild steel pressure vessel," *Journal of Zhejiang University Science A,* pp. 277-281, 2006.

[20] N. Ihn and H. G. Nguyen, "Investigation of burst pressures in PWR primary pressure boundary components," *Nuclear Engineering and Technology,* Vol. 48, pp. 236-245, 2016.

[21] M. Muscat, D. Mackenzie and R. Hamilton, "A work criterion for plastic collapse," *International Journal of Pressure Vessels and Piping,* Vol. 80, pp. 49-58, 2003.

[22] M. F. Shi and J. C. Gerdeen, "Effect of strain gradient and curvature on forming limit diagrams for anisotropic sheets," *Journal of Materials Shaping Technology,* Vol. 9, pp. 253-268, 1991.

[23] American Petroleum Institute, API Specification 5L, *Line Pipe*, 46th ed. 2020.

[24] J. Yang and S. Hu, "Estimation of burst pressure of PVC pipe using average shear stress yield criterion: Experimental and numerical studies," *Applied Sciences,* Vol. 11, p. 10477, 2021.

[25] F. Jiang and E. Zhao, "An integrated risk analysis model for corroded pipelines subjected to internal pressures: Considering the interacting effects," *Ocean Engineering,* Vol. 247, p. 110683, 2022.

[26] L. B. Turner, "The stresses in a thick hollow cylinder subjected to internal pressure," *Transactions of Cambridge Philosophical Society,* Vol. 21, pp. 377-396, 1910.

[27] J. Kiefner, W. Maxey and A. Duffy, "The significance of the yield-to-ultimate strength ratio of line pipe materials," Summary report to Pipeline Research Committee, American Gas Association, 1971.

[28] S. Papka, J. Stevens, M. Macia, D. Fairchild and C. Petersen, "Full-size testing and analysis of X120 linepipe," *International Journal of Offshore and Polar Engineering,* Vol. 14, pp. 42-51, 2004.

[29] M. Law, G. Bowie and L. Fletcher, "Pipeline behaviour, the hydrostatic strength test and failure strain," in *Proceedings of the 15th conference of PRCI and EPRG pipeline conference*, Orlando, FL, 2005.

[30] P. Paslay, E. Cernocky and R. Wink, "Burst pressure prediction on thin-walled, ductile tubulars subjected to axial load," in *Proceedings of applied technology workshop on risk based design of well cashing and tubing*, Woodlands, TX, 1998.

[31] W. Maxey, "Y/T significance in line pipe," in *Proccedings of the seventh symposium on line pipe research*, Houston, TX, 1986.

[32] D. Mok, R. Pick, A. Glover and R. Hoff, "Bursting of line pipe with long external corrosion," *International Journal of Pressure Vessels and Piping,* Vol. 46, pp. 195-216, 1991.

[33] B. Chouchaoui, *Evaluating the Remaining Strength of Corroded Pipelines*,Ph.D Thesis, Department of Mechanical Engineering, University of Waterloo, Canada, 1993.

[34] K. Amano, M. Matsuoka, T. Ishihara, K. Tanaka, T. Inoue, Y. Kawaguchi and M. Tsukamoto, "Significance of yield ratio limitation to plastic deformation of pipeline in high pressure proof test," in *Proceedings of the seventh symposium on line pipe research*, Houston TX, 1986.

[35] H. Hillenbrand, A. Liessem, G. Knauf, K. Niederhoff and J. Bauer, "Development of large-diameter pipe in grade X100," in *Proceedings of the Third International Conference of Pipeline Technology*, Brugge, Belgium, 2000.

[36] A. Liessem, M. Graef, G. Knauf and U. Marewski, "Influence of thermal treatment on mechanical properties of UOE linepipe," in *4th International Conference on Pipeline Technology*, Ostend, Belgium, 2004.

[37] S. Okaguchi, H. Makino, M. Hamada, A. Yamamoto, T. Ikeda, I. Takeuchi, D. Fairchild, M. Macia, S. Papka, J. Stevens and et. al., "Development and mechanical properties of X120 linepipe," *International Journal of Offshore and Polar Engineering,* Vol. 14, pp. 28-35, 2004.

[38] T. Netto, U. Ferraz and S. Estefen, "The effect of corrosion defects on the burst pressure of pipelines," *Journal of Constructional Steel Research,* Vol. 61, pp. 1185-1204, 2005.

Appendix A – Burst Pressure Data

Table A1. Comparison of Eq. (9) to FEA predicted Zhu-Leis and Svensson burst pressures.

Steel grade	OD (in)	WT (in)	YS (ksi)	UTS (ksi)	FEA P_b (psi)	Proposed Model (psi)	% Error	Svensson Model (psi)	% Error
Grade B	42	0.50	35.678	60.200	1388	1387	0.03	1440	3.76
Grade B	30	0.25	35.678	60.200	968	967	0.03	1004	3.76
Grade B	30	0.50	35.678	60.200	1952	1952	0.04	2026	3.75
Grade B	30	0.75	35.678	60.200	2953	2953	0.02	3065	3.77
Grade B	24	0.25	35.678	60.200	1212	1212	0.04	1258	3.75
Grade B	24	0.50	35.678	60.200	2451	2450	0.03	2543	3.76
Grade B	24	1.00	35.678	60.200	5008	5009	-0.02	5199	3.81
Grade B	16	0.50	35.678	60.200	3715	3715	0.00	3856	3.79
Grade B	16	0.75	35.678	60.200	5664	5667	-0.04	5881	3.84
Grade B	8	0.50	35.678	60.200	7679	7687	-0.10	7978	3.90
Grade B	8	0.75	35.678	60.200	11916	11953	-0.31	12406	4.11
Grade B	8	1.00	35.678	60.200	16453	16560	-0.65	17188	4.47
X52	42	0.50	52.462	66.700	1616	1620	-0.23	1696	4.89
X52	30	0.25	52.462	66.700	1127	1130	-0.23	1183	4.89
X52	30	0.50	52.462	66.700	2274	2279	-0.23	2385	4.89
X52	30	0.75	52.462	66.700	3440	3449	-0.25	3609	4.91
X52	24	0.25	52.462	66.700	1412	1416	-0.22	1481	4.88
X52	24	0.50	52.462	66.700	2855	2861	-0.24	2994	4.90
X52	24	1.00	52.462	66.700	5833	5850	-0.29	6122	4.95
X52	16	0.50	52.462	66.700	4328	4339	-0.26	4541	4.92
X52	16	0.75	52.462	66.700	6599	6619	-0.30	6926	4.96
X52	8	0.50	52.462	66.700	8944	8978	-0.38	9395	5.04
X52	8	0.75	52.462	66.700	13880	13961	-0.58	14609	5.26
X52	8	1.00	52.462	66.700	19165	19342	-0.92	20241	5.61
X80	42	0.50	80.904	90.600	2255	2261	-0.26	2378	5.44
X80	30	0.25	80.904	90.600	1573	1577	-0.26	1658	5.44
X80	30	0.50	80.904	90.600	3172	3181	-0.26	3345	5.45
X80	30	0.75	80.904	90.600	4799	4812	-0.27	5061	5.45
X80	24	0.25	80.904	90.600	1970	1975	-0.26	2077	5.44
X80	24	0.50	80.904	90.600	3982	3993	-0.27	4199	5.45
X80	24	1.00	80.904	90.600	8137	8163	-0.32	8585	5.50
X80	16	0.50	80.904	90.600	6038	6055	-0.29	6368	5.47
X80	16	0.75	80.904	90.600	9204	9235	-0.34	9713	5.52
X80	8	0.50	80.904	90.600	12477	12528	-0.40	13175	5.59

X80	8	0.75	80.904	90.600	19361	19480	-0.61	20487	5.81